AN3059
Rev. 0, 1/2006

Channel Estimation in OFDM Systems

by Yushi Shen and Ed Martinez

This application note gives an overview of the channel estimation strategies used in orthogonal frequency division multiplexing (OFDM) systems. **Section 1** describes the protocols associated with OFDM systems and the problems posed by such systems. **Section 2** through **Section 5** describe the various types of channel estimation methods for use in such systems. The implementation complexity and system performance of the methods are studied and compared in **Section 6**, measuring performance in terms of symbol error rate (SER).

CONTENTS

freescale semiconductor

1 OFDM Background

OFDM is becoming widely applied in wireless communications systems due to its high rate transmission capability with high bandwidth efficiency and its robustness with regard to multi-path fading and delay [1]. It has been used in digital audio broadcasting (DAB) systems, digital video broadcasting (DVB) systems, digital subscriber line (DSL) standards, and wireless LAN standards such as the American **IEEE**® Std. 802.11™ (WiFi) and its European equivalent HIPRLAN/2. It has also been proposed for wireless broadband access standards such as **IEEE** Std. 802.16™ (WiMAX) and as the core technique for the fourth-generation (4G) wireless mobile communications.

The use of differential phase-shift keying (DPSK) in OFDM systems avoids need to track a time varying channel; however, it limits the number of bits per symbol and results in a 3 dB loss in signal-to-noise ratio (SNR). Coherent modulation allows arbitrary signal constellations, but efficient channel estimation strategies are required for coherent detection and decoding.

There are two main problems in designing channel estimators for wireless OFDM systems. The first problem is the arrangement of pilot information, where pilot means the reference signal used by both transmitters and receivers. The second problem is the design of an estimator with both low complexity and good channel tracking ability. The two problems are interconnected. In general, the fading channel of OFDM systems can be viewed as a two-dimensional (2D) signal (time and frequency). The optimal channel estimator in terms of mean-square error is based on 2D Wiener filter interpolation. Unfortunately, such a 2D estimator structure is too complex for practical implementation. The combination of high data rates and low bit error rates in OFDM systems necessitates the use of estimators that have both low complexity and high accuracy, where the two constraints work against each other and a good trade-off is needed. The one-dimensional (1D) channel estimations are usually adopted in OFDM systems to accomplish the trade-off between complexity and accuracy [1–7]. The two basic 1D channel estimations are block-type pilot channel estimation and comb-type pilot channel estimation, in which the pilots are inserted in the frequency direction and in the time direction, respectively. The estimations for the block-type pilot arrangement can be based on least square (LS), minimum mean-square error (MMSE), and modified MMSE. The estimations for the comb-type pilot arrangement includes the LS estimator with 1D interpolation, the maximum likelihood (ML) estimator, and the parametric channel modeling-based (PCMB) estimator. Other channel estimation strategies were also studied [8–12], such as the estimators based on simplified 2D interpolations, the estimators based on iterative filtering and decoding, estimators for the OFDM systems with multiple transmit-and-receive antennas, and so on.

2 Baseband Model

The basic idea underlying OFDM systems is the division of the available frequency spectrum into several subcarriers. To obtain a high spectral efficiency, the frequency responses of the subcarriers are overlapping and orthogonal, hence the name OFDM. This orthogonality can be completely maintained with a small price in a loss in SNR, even though the signal passes through a time dispersive fading channel, by introducing a cyclic prefix (CP). A block diagram of a baseband OFDM system is shown in **Figure 1**.

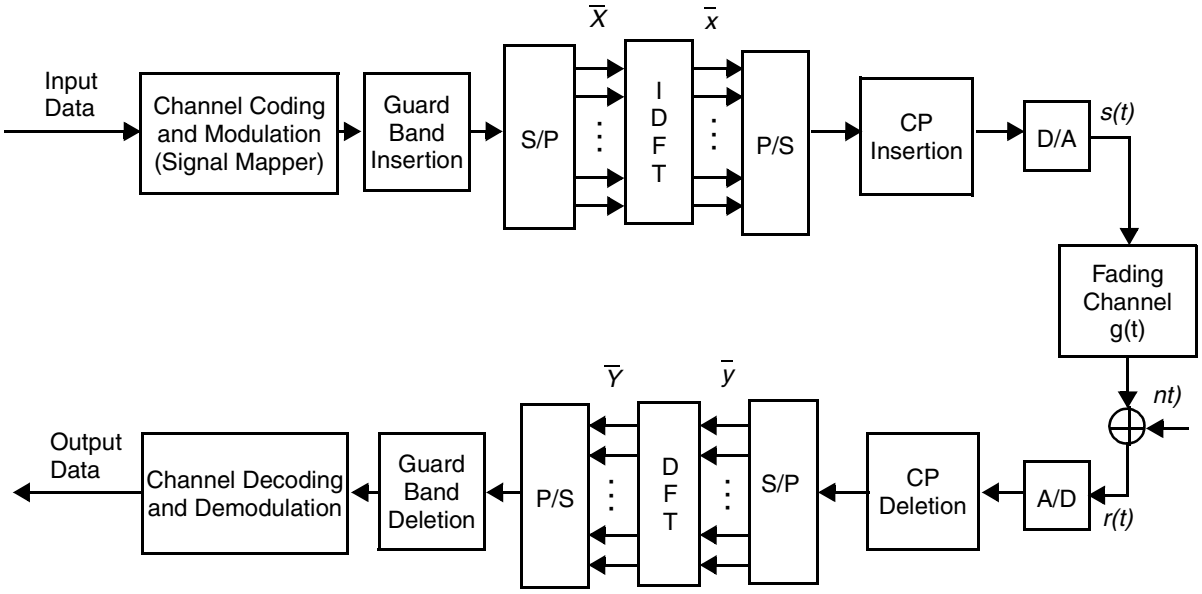

Figure 1. A Digital Implementation of a Baseband OFDM System.

The binary information is first grouped, coded, and mapped according to the modulation in a "signal mapper." After the guard band is inserted, an N-point inverse discrete-time Fourier transform ($IDFT_N$) block transforms the data sequence into time domain (note that N is typically 256 or larger). Following the IDFT block, a cyclic extension of time length T_G, chosen to be larger than the expected delay spread, is inserted to avoid intersymbol and intercarrier interferences. The D/A converter contains low-pass filters with bandwidth $1/T_S$, where T_S is the sampling interval. The channel is modeled as an impulse response g(t) followed by the complex additive white Gaussian noise (AWGN) n(t), where α_m is a complex values and $0 \leq \tau_m T_S \leq T_G$.

$$g(t) = \sum_{m=1}^{M} \alpha_m \delta(t - \tau_m T_S) \qquad \textbf{Equation 1}$$

At the receiver, after passing through the analog-to-digital converter (ADC) and removing the CP, the DFT_N is used to transform the data back to frequency domain. Lastly, the binary information data is obtained back after the demodulation and channel decoding.

Let $\bar{X} = [X_k]^T$ and $\bar{Y} = [Y_k]^T \quad (k = 0, \ ..., N-1)$ denote the input data of IDFT block at the transmitter and the output data of DFT block at the receiver, respectively. Let $\bar{g} = [g_n]^T$ and $\bar{n} = [n_n]^T \quad (n = 0, \ ..., N-1)$ denote the sampled channel impulse response and AWGN, respectively. Define the input matrix $\underline{X} = diag(\bar{X})$ and the DFT-matrix,

$$\underline{F} = \begin{bmatrix} W_N^{00} & \cdots & W_N^{0(N-1)} \\ & \ddots & \\ W_N^{(N-1)0} & \cdots & W_N^{(N-1)(N-1)} \end{bmatrix} \qquad \textbf{Equation 2}$$

where $W_N^{i,k} = (1/\sqrt{N})^{-j2\Pi(ik/N)}$. Also define $\bar{H} = DFT_N(\bar{g}) = \underline{F}\bar{g}$, and $\bar{N} = \underline{F}\bar{n}$.

Under the assumption that the interferences are completely eliminated [1–3], you can derive:

$$\bar{Y} = DFT_N(IDFT_N(\bar{X}) \otimes \bar{g} + \bar{n}) = \underline{X}\underline{F}\bar{g} + \bar{N} = \underline{X}\bar{H} + \bar{N} \quad \textbf{Equation 3}$$

This equation demonstrates that an OFDM system is equivalent to a transmission of data over a set of parallel channels.

As a result, the fading channel of the OFDM system can be viewed as a 2D lattice in a time-frequency plane, which is sampled at pilot positions and the channel characteristics between pilots are estimated by interpolation. The art in designing channel estimators is to solve this problem with a good trade-off between complexity and performance.

The two basic 1D channel estimations in OFDM systems are illustrated in **Figure 2**. The first one, block-type pilot channel estimation, is developed under the assumption of slow fading channel, and it is performed by inserting pilot tones into all subcarriers of OFDM symbols within a specific period. The second one, comb-type pilot channel estimation, is introduced to satisfy the need for equalizing when the channel changes even from one OFDM block to the subsequent one. It is thus performed by inserting pilot tones into certain subcarriers of each OFDM symbol, where the interpolation is needed to estimate the conditions of data subcarriers. The strategies of these two basic types are analyzed in the next sections.

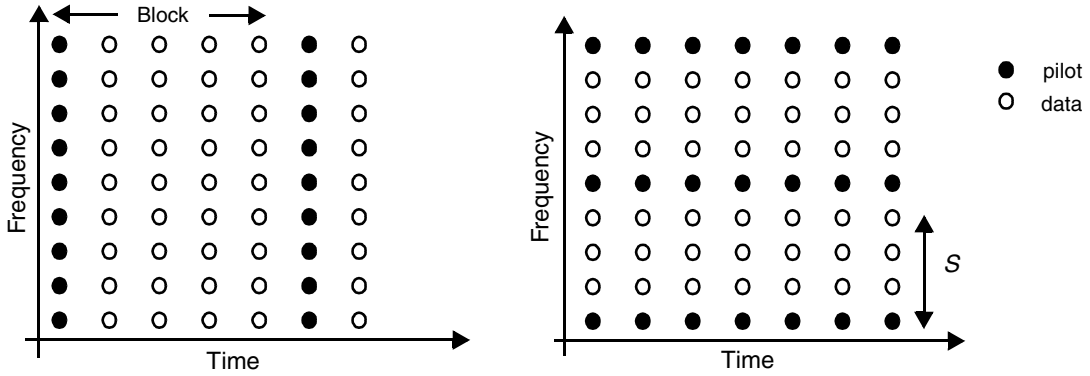

Figure 2. Two Basic Types of Pilot Arrangement for OFDM Channel Estimations

3 Block-Type Pilot Channel Estimation

In block-type pilot-based channel estimation, as shown in **Figure 2**, OFDM channel estimation symbols are transmitted periodically, and all subcarriers are used as pilots. The task here is to estimate the channel conditions (specified by $\bar{H}$ or $\bar{g}$) given the pilot signals (specified by matrix $\underline{X}$ or vector $\bar{X}$) and received signals (specified by $\bar{Y}$), with or without using certain knowledge of the channel statistics. The receiver uses the estimated channel conditions to decode the received data inside the block until the next pilot symbol arrives. The estimation can be based on least square (LS), minimum mean-square error (MMSE), and modified MMSE.

3.1 LS Estimator

The LS estimator minimizes the parameter $(\bar{Y} - \underline{X}\bar{H})^H(\bar{Y} - \underline{X}\bar{H})$, where $(\bullet)^H$ means the conjugate transpose operation. It is shown that the LS estimator of $\bar{H}$ is given by [2].

$$\hat{H}_{LS} = \underline{X}^{-1}\bar{Y} = [(X_k / Y_k)]^T \qquad (k = 0, ..., N-1) \quad \textbf{Equation 4}$$

Without using any knowledge of the statistics of the channels, the LS estimators are calculated with very low complexity, but they suffer from a high mean-square error.

3.2 MMSE Estimator

The MMSE estimator employs the second-order statistics of the channel conditions to minimize the mean-square error.

Denote by $\underline{R}_{gg}$, $\underline{R}_{HH}$, and $\underline{R}_{YY}$ the autocovariance matrix of $\bar{g}$, $\bar{H}$, and $\bar{Y}$, respectively, and by $\underline{R}_{gY}$ the cross covariance matrix between $\bar{g}$ and $\bar{Y}$. Also denote by σ_N^2 the noise variance $E\{|\bar{N}|^2\}$. Assume the channel vector $\bar{g}$ and the noise $\bar{N}$ are uncorrelated, it is derived that

$$\underline{R}_{HH} = E\{\bar{H}\bar{H}^H\} = E\{(\underline{F}\bar{g})(\underline{F}\bar{g})^H\} = \underline{F}\underline{R}_{gg}\underline{F}^H \quad \text{Equation 5}$$

$$\underline{R}_{gY} = E\{\bar{g}\bar{Y}^H\} = E\{\bar{g}(\underline{X}\underline{F}\bar{g} + \bar{N})^H\} = \underline{R}_{gg}\underline{F}^H\underline{X}^H \quad \text{Equation 6}$$

$$\underline{R}_{YY} = E\{\bar{Y}\bar{Y}^H\} = \underline{X}\underline{F}\underline{R}_{gg}\underline{F}^H\underline{X}^H + \sigma_N^2\underline{I}_N \quad \text{Equation 7}$$

Assume $\underline{R}_{gg}$ (thus $\underline{R}_{HH}$) and σ_N^2 are known at the receiver in advance, the MMSE estimator of $\bar{g}$ is given by $\hat{g}_{MMSE} = \underline{R}_{gY}\underline{R}_{YY}^{-1}\bar{Y}^{HH}$ [2–5]. Note that if $\bar{g}$ is not Gaussian, $\hat{g}_{MMSE}$ is not necessarily a minimum mean-square error estimator, but it is still the best linear estimator in the mean-square error sense. At last, it is calculated that

$$\begin{aligned}\hat{H}_{MMSE} &= \underline{F}\hat{g}_{MMSE} = \underline{F}[(\underline{F}^H\underline{X}^H)^{-1}\underline{R}_{gg}^{-1}\sigma_N^2 + XF]^{-1}\bar{Y} \\ &= \underline{F}\underline{R}_{gg}[(\underline{F}^H\underline{X}^H\underline{X}\underline{F})^{-1}\sigma_N^2 + \underline{R}_{gg}]\underline{F}^{-1}\hat{H}_{LS} \\ &= \underline{R}_{HH}[\underline{R}_{HH} + \sigma_N^2(\underline{X}\underline{X}^H)^{-1}]^{-1}\hat{H}_{LS}\end{aligned} \quad \text{Equation 8}$$

The MMSE estimator yields much better performance than LS estimators, especially under the low SNR scenarios. A major drawback of the MMSE estimator is its high computational complexity, especially if matrix inversions are needed each time the data in $\underline{X}$ changes.

3.3 Modified MMSE Estimator

Modified MMSE estimators are studied widely to reduce complexity [2–4]. Among them, an optimal low-rank MMSE (OLR-MMSE) estimator is proposed in this paper, which combines the following three simplification techniques:

1. The first simplification of MMSE estimator is to replace the term $(\underline{X}\underline{X}^H)^{-1}$ in **Equation 8** with its expectation $E\{(\underline{X}\underline{X}^H)^{-1}\}$. Assuming the same signal constellation on all tones and equal probability on all constellation points, we have

$$E\{(\underline{X}\underline{X}^H)^{-1}\} = E\{|1/X_k|^2\}\underline{I} \quad \text{Equation 9}$$

Defining the average SNR as $\overline{SNR} = E\{|X_k|^2\}/\sigma_N^2$, and the term $\beta = E\{|X_k|^2\}/E\{|1/X_k|^2\}$. The term $\sigma_N^2(\underline{X}\underline{X}^H)^{-1}$ is then approximate by $(\beta/\overline{SNR})\underline{I}$, where β is a constant depending only on the signal constellation. For example, for a 16-QAM transmission, $\beta = 17/9$.

2. The second simplification is based on the low-rank approximation. As indicated in **Section 2** that **Equation 1** has $0 \le \tau_m T_S \le T_G$, most of the energy in $\bar{g}$ is contained in, or near, the first $(L+1)$ taps, where $L = \lceil T_G / T_S \rceil N$ and N is the DFT size. Therefore, we can only consider the taps with significant energy, that is, the upper left corner of the autocovariance matrix $\underline{R}_{gg}$. In the **IEEE** Std. 802.11 and **IEEE** Std. 802.16 [13], $\lceil T_G / T_S \rceil$ is chosen among {1/32, 1/16, 1/8, 1/4}, so the effective size of matrix is reduced dramatically after the low-rank approximation is used.
3. The third simplification uses the singular value decomposition (SVD). The SVD of $\underline{R}_{HH}$ is $\underline{R}_{HH} = \underline{U}\underline{\Lambda}\underline{U}^H$, where $\underline{U}$ is a unitary matrix containing the singular vectors and Λ is a diagonal matrix containing the singular values $\lambda_0 \ge \lambda_1 \ge \ldots \ge \lambda_{N-1}$ on its diagonal. The SVD also dramatically reduces the calculation complexity of matrices.

Combining all simplification techniques, the OLR-MMSE estimator is explained as follows. The system first determines the number of ranks required by the estimator, denoted by p, which should be no smaller than $(L+1)$. Then, given the signal constellation, the noise variance and the channel autocovariance matrix $\underline{R}_{HH}$, the receiver pre-calculates β, $\overline{SNR}$, the unitary matrix $\underline{U}$, and the singular values λ_ks. It thus obtains the $(N \times N)$ diagonal matrix $\underline{\Delta}_p$ with entries

$$\delta_k = \begin{cases} \left[\lambda_k / \left(\lambda_k + \dfrac{\beta}{\overline{SNR}}\right)\right], & k = 0, 1, \ldots, p-1 \\ 0, & k = p, \ldots, N-1 \end{cases} \qquad \textbf{Equation 10}$$

During the transmission, using the transmitted pilots $\underline{X}$ and received signals $\bar{Y}$, the $\hat{H}_{LS}$ is calculated according to **Equation 4**, and the OLR-MMSE estimator with rank p is given by

$$\hat{H}_{OLR-MMSE} = \underline{U}\underline{\Delta}_p\underline{U}^H\hat{H}_{LS} \qquad \textbf{Equation 11}$$

The OLR-MMSE estimator can be interpreted as first projecting the LS estimates onto a subspace and then performing the estimation. Because the subspace has a small dimension (as small as $(L+1)$ and still describes the channel well, the complexity of OLR-MMSE estimator is much lower than MMSE estimator with a good performance. However, the low-rank estimators introduce an irreducible error floor due to the part of the channel that does not belong to the subspace. A legitimate question is what if $(L+1)$ is too large to deal with—for example, if the DFT size N is 2048, and $\lceil T_G / T_S \rceil$ is 1/4, $(L+1)$ is still as large as 513. One solution to this problem is to partition the tones into reasonably-sized blocks and perform the estimation independently in these blocks. For example, the 2048-tone system can be approximately described by 32 parallel 64-tone systems, and each channel attenuation can be estimated independently by OLR-MMSE estimator with rank $p = (64/4 + 1) = 17$. In the scenarios when $(L+1)$ is large, this strategy reduces the complexity significantly at the expense of certain performance loss because it neglects the correlation between tones in different subsystems.

3.4 Estimation with Decision Feedback

In block-type pilot-based channels, the estimators are usually calculated once per block and are used until the next pilot symbol arrives. The channel estimation with decision feedback is proposed to improve the performance, where the estimators inside the block are updated using the decision feedback equalizer at each subcarrier. The receiver first estimates the channel conditions using the pilots and obtains $\hat{H} = \{\hat{H}_k\}\ (k = 0, \ldots, N-1)$, which is based on LS, MMSE, or modified MMSE. Inside the block, for each coming symbol and for its each subcarrier, the estimated transmitted signal is found by the previous $\hat{H}_k$ according to the formula $\hat{X}_k = Y_k / \hat{H}_k$. $\{\hat{X}_k\}$ is mapped to the binary data through the demodulation according to the "signal demapper," and then obtained back though "signal mapper" as $\{\tilde{X}_k\}$. The estimated channel $\hat{H}_k$ is updated by $\hat{H}_k = Y_k / \tilde{X}_k$ and is used in the next symbol.

Note: The block-type channel estimation is suitable for slow fading channels; the fast fading channel causes the complete loss of estimated channel parameters.

4 Comb-Type Pilot Channel Estimation

In comb-type pilot based channel estimation, as shown in **Figure 2**, for each transmitted symbol, N_p pilot signals are uniformly inserted into $\overline{X}$ with S with subcarriers apart from each other, where $S = N/N_p$.

The receiver knows the pilots locations $\overline{P} = [P_k]^T$ $(k = 0, ..., N_p - 1)$, the pilot values $\overline{X}^p = [X_k^p]^T$ $(k = 0, ..., N_p - 1)$, and the received signal $\overline{Y}$. The LS estimates to the channel conditions at the pilot subcarriers $(\overline{H}^p)$ are calculated by

$$\hat{H}_{LS}^p = [Y(P_o)/X_0^p, Y(P_1)/X_1^p, ..., Y(P_{Np-1})/X_{Np-1}^p]^T \quad \text{Equation 12}$$

The task here is to estimate the channel conditions at the data subcarriers (specified by $\overline{H}$ with length N), given the LS estimates at pilot subcarriers $\hat{H}_{LS}^p$, received signals $\overline{Y}$, and maybe certain additional knowledge of the channel statistics. The solutions include LS estimator with 1D interpolation, the maximum likelihood (ML) estimator, and the parametric channel modeling-based (PCMB) estimator. [5–7].

4.1 LS Estimator with 1D Interpolation

1D interpolation is used to estimate the channel at data subcarriers, where the vector $\hat{H}_{LS}^p$ with length N_p is interpolated to the vector $\hat{H}$ with length N, without using additional knowledge of the channel statistics. The 1D interpolation methods are summarized in the remainder of this section.

4.1.1 Linear Interpolation (LI)

The LI method performs better than the piecewise-constant interpolation, where the channel estimation at the data subcarrier between two pilot $\hat{H}_{LS}^p(k)$ and $\hat{H}_{LS}^p(k+1)$ is given by:

$$\hat{H}(kS + t) = \hat{H}_{LS}^p(k) + (\hat{H}_{LS}^p(k+1) - \hat{H}_{LS}^p(k))(t/S) \qquad (0 \le t \le S) \quad \text{Equation 13}$$

4.1.2 Second-Order Interpolation (SOI)

The SOI method performs better than the LI method, where the channel estimation at the data subcarrier is obtained by weighted linear combination of the three adjacent pilot estimates.

4.1.3 Low-Pass Interpolation (LPI)

The LPI method is performed by inserting zeros into the original $\hat{H}_{LS}^p$ sequence and then applying a low-pass finite-length impulse response (FIR) filter (the *interp* function in MATLAB), which allows the original data to pass through unchanged. This method also interpolates such that the mean-square error between the interpolated points and their ideal values is minimized.

4.1.4 Spline Cubic Interpolation (SCI)

The SCI method produces a smooth and continuous polynomial fitted to given data points (the *spline* function in MATLAB).

4.1.5 Time Domain Interpolation (TDI)

The TDI method is a high-resolution interpolation based on zero-padding and DFT/IDFT. It first converts $\hat{H}_{LS}^{p}$ to time domain by IDFT and then interpolate the time domain sequence to N points with simple piecewise-constant method [5]. Finally, the DFT converts the interpolated time domain sequence back to the frequency domain.

In [5], the performance among these estimation techniques usually ranges from the best to the worst, as follows: LPI, SCI, TDI, SOI, and LI. Also, LPI and SCI yield almost the same best performance in the low and middle SNR scenarios, while LPI outperforms SCI at the high SNR scenario. In terms of the complexity, TDI, LPI and SCI have roughly the same computational burden, while SOI and LI have less complexity. As a result, LPI and SCI are usually recommended because they yield the best trade-off between performance and complexity.

4.2 ML Estimator

As mentioned in **Section 3.3**, most of the energy in $\bar{g}$ is contained in, or near, the first $(L+1)$ taps, where $L = \lceil T_G / T_S \rceil N$. Define $\bar{g}_{L+1} = [g_0, ..., g_{L+1}]^T$ is the first $(L+1)$ taps of $\bar{g}$. Similarly to the definition of the square DFT matrix $\underline{F}$, we define the non-square DFT matrix

$$\underline{F}_{A,B} = [W_N^{a,b}]_{A \times B} \qquad (0 \le a < A,\ 0 \le b < B) \qquad \textbf{Equation 14}$$

Also, we define the uniform-spaced-DFT matrix with space S as follows:

$$\underline{F}(S)_{A,B} = [W_N^{aS,b}]_{A \times B} = [W_N^{a,bS}]_{A \times B} \qquad (0 \le a < A,\ 0 \le b < B) \qquad \textbf{Equation 15}$$

It is obvious that $\bar{H}^{p} = \underline{F}(S)_{Np \times (L+1)} \bar{g}_{L+1}$, where S is the space between pilot subcarriers. Thus, the maximum likelihood estimator (MLE) of $\bar{g}_{L+1}$ given the estimate to $\bar{H}p$ (we use $\hat{H}_{LS}^{p}$) is obtained by

$$\bar{g}_{L+1} = (\underline{F}(S)_{Np,(L+1)}^{H} \times \underline{F}(S)_{Np,(L+1)})^{-1} (\underline{F}(S)_{Np,(L+1)}^{H}) \hat{H}_{LS}^{p} \qquad \textbf{Equation 16}$$

Finally, the complete channel estimate $\hat{H}$ of all the subcarriers is computed from $\bar{g}_{L+1}$ by

$$\hat{H}_{MLE} = \underline{F}_{N,(L+1)} \hat{g}_{L+1} \qquad \textbf{Equation 17}$$

4.3 PCMB Estimator

As shown in **Equation 1**, the channel is modeled by a multipath fading channel with M resolvable paths with different path complex gain $\{\alpha_m\}$ and time delays $\{\tau_m T_S\}$. We assume different path gains are uncorrelated with respect to each other and denoted by $R_\alpha(M)$ the channel auto-covariance matrix, and $R_\alpha(M) = diag\{\sigma_{\alpha 1}^2, ..., \sigma_{\alpha M}^2\}$. In [7], a channel estimation scheme based on the parametric channel modeling is proposed. In this estimator, knowledge of the channel is required; that is, M, and $\{\tau_m T_S\}$ are required. The estimate of M, denoted by $\hat{M}$, is obtained by the criterion of minimum description length (MDL). The estimation of signal parameters by rotational invariance (ESPRIT) [8] method is used to acquire the initial multipath time delays, and an inter-path interference cancellation (IPIC) delay locked loop (DLL) tracks the channel multipath time delays. We define two nonuniform-spaced-DFT matrices as follows:

$$\underline{B}_{Np,\hat{M}} = [W_N^{P(k),\hat{\tau}(m)}]_{Np \times \hat{M}} \qquad (0 \le k < N_p,\ 1 \le m \le \hat{M}) \qquad \textbf{Equation 18}$$

$$\underline{B}_{N,\hat{M}} = [W_N^{i,\hat{\tau}(m)}]_{N \times \hat{M}} \qquad (0 \le i < N,\ 0 \le m \le \hat{M}) \qquad \textbf{Equation 19}$$

where $\{P(k)\}$ are the pilot locations, and $\{\hat{\tau}(m)\}$ are the estimated multipath time delays. The MMSE estimator is given by [5]:

$$\hat{H}_{PCMB} = \underline{B}_{Np,\hat{M}} \times \left(\frac{\gamma}{\overline{SNR}} R_{\alpha}(\hat{M})^{-1} + \underline{B}^{H}_{Np,\hat{M}} \underline{B}_{Np,\hat{M}} \right)^{-1} \times \underline{B}^{H}_{Np,\hat{M}} \times \hat{H}^{p}_{LS} \qquad \text{Equation 20}$$

where $\overline{SNR}$ is the average SNR, and γ is the ratio of average signal power to the pilot power.

When these three channel estimation schemes are compared, the LS estimator with 1D interpolation shows the lowest complexity. Without counting the complexity of the MDL scheme and IPIC-DLL to track the channel parameters, the PCMB estimator is usually simpler than the ML estimator, if $2\hat{M} < N_p$ [6]. Also, the LS estimator with 1D interpolation scheme is worse than the other two in terms of both MSE and SER. The performance of the PCMB estimator and ML estimator i almost the same, though the former performs slightly better in MSE at small SNRs.

5 Other Pilot-Aided Channel Estimations

Other channel estimation schemes include the simplified 2D channel estimators, the iterative channel estimators, and the channel estimators for the OFDM systems with multiple transmit-and-receive antennas.

5.1 Simplified 2D Estimators

In 2D channel estimation, the pilots are inserted in both the time and frequency domains, and the estimators are based on 2D filters. In general, 2D channel estimation yields better performance than the 1D scheme, at the expense of higher computational complexity and processing delay. The optimal solution in terms of mean-square error is based on 2D Wiener filter interpolation, which employs the second-order statistics of the channel conditions. However, such a 2D estimator structure suffers from a huge computational complexity, especially when the DFT size N is several hundred or larger. A proposed algorithm with two concatenated 1D linear interpolations on frequency and time sequentially minimizes the system complexity. In [9], channel estimators based on 2D least square (LS) and 2D normalized least square (NLS) are proposed, and a parallel 2D (N)LS channel estimation scheme solves the realization problem due to the high computational complexity of 2D adaptive channel estimation.

5.2 Iterative Channel Estimators

Two efficient iterative channel estimators are proposed in [10]. To reduce complexity, the 2D transmission lattice is divided by 2D blocks, and the pilots are uniformly inserted inside each block. Channel estimation proceeds on a block-by-block basis. The first estimator is based on iterative filtering and decoding, which consists of two cascaded 1D Wiener filters to interpolate the unknown time-varying 2D frequency response between the known pilot symbols. The second estimator uses an *a posteriori* probability (APP) algorithm, in which the two APP estimators, one for the frequency and the other for the time direction, are embedded in an iterative loop similar to the turbo decoding principle. These iterative estimators yield robust performance even at low SNR scenarios, but with high computation complexity and certain iteration time delay.

5.3 Channel Estimators for OFDM with Multiple Antennas

Multiple transmit-and-receive antennas in OFDM systems can improve communication quality and capacity. For the OFDM systems with multiple transmit antennas, each tone at each receiver antenna is associated with multiple channel parameters, which makes channel estimation difficult. Fortunately, channel parameters for different tones of each channel are correlated and the channel estimators are based on this correlation.

Several channel estimation schemes have been proposed for the OFDM systems with multiple transmit-and-receive antennas for space diversity, or multiple input multiple output (MIMO) systems for high-rate wireless data access. For example, in [11], channel estimation is based on a 1D block-type pilot arrangement, and optimal training sequences are constructed not only to optimize, but also to simplify channel estimation during the training period. In [12], channel estimation in 2Ds for OFDM systems with multiple transmit antennas is discussed. The approach estimates and separates N_T superimposed received signals, corresponding to N_T transmit antennas, by exploiting the correlation in 2D of the received signal. More specifically, it uses two 1D estimators instead of a true 2D estimator, by dividing the estimation and the separation task into two stages. The first stage separates a subset of the superimposed signals and estimates the channel response in the first dimension. The second stage further separates the signals of each subset in the second dimension, yielding an estimate for all transmit antennas. For space-time block-coded OFDM systems, this proposed estimator can track the channel variations even at high Doppler frequencies.

6 Performance Evaluation

This section summarizes the computational complexity of the proposed channel estimation schemes and provides simulation results to demonstrate performance.

6.1 Complexity Analysis

In general, 1D channel estimation schemes have a much lower computational complexity than 2D schemes because they avoid computing 2D matrices. Also, block-type pilot-channel estimation schemes are usually simpler than comb-type pilot schemes because they calculate the estimators once per block. In the block-type pilot schemes with decision feedback, the estimators are updated for each symbol by simple vector division. Com-type pilot schemes calculate the estimators for every OFDM symbol. Algorithm complexity, ranking from low to high, is summarized in **Table 1** and **Table 2** for the block-type pilot arrangement and comb-type pilot arrangement, respectively.

Table 1. Computational Complexity Analysis: Channel Estimation Schemes with Block-Type Pilot Arrangement

Estimation Scheme	Complexity	Comments
LS Estimator	Low	Simple vector division.
OLR-MMSE Estimator	Moderate	Avoid matrix inversion and also simplify the matrix operations to the calculations between a low-rank diagonal matrix and a unitary matrix.
MMSE Estimator	High	Matrix inversion and other operations with size *N*, where *N* is the DFT size (typically 256, 512, 1024, or 2048).

Table 2. Computational Complexity Analysis: Channel Estimation Schemes with Comb-Type Pilot Arrangement

Estimation Scheme		Complexity	Comments
LS Estimator with 1D interpolation	LI	Lowest	Simple estimation and interpolation methods.
	SOI	Low	
	SCI	Moderate	Interpolation methods are relatively complex, with fitted polynomial search, low-pass convolution, and DFT/IDFT calculation, respectively.
	LPI		
	TDI		
ML Estimator		High	Matrix inversion with size (L + 1), where L ranges from N/32 to N/4, and other matrix operations with size N.
PCMB Estimator		High	Tracking the number of resolvable paths (M) and channel delays, and matrix inversion with size M, and other matrix operations with size N.

6.2 Simulation Performance

In general, the 2D channel estimation schemes outperform the 1D schemes by exploiting the 2D correlations at the expense of higher computational complexity and larger time delay. Also, the block-type pilot channel estimation schemes are more suitable for the slow fading channels, and the comb-type pilot channel estimation schemes are more suitable for the middle and fast fading channels. In addition, block-type pilot schemes are used over middle or fasting fading channels, the channel estimation error may vary considerably as a function of the location of the data blocks with respect to the pilot block. The result may be a periodic variation of the decoding error rates for different OFDM blocks. On the other hand, the comb-type pilot schemes can eliminate this variation, and therefore all OFDM data symbols experience a similar error rate. Because the error rate of the comb-type pilot schemes is higher than the lowest error rate that can be achieved by the block-type pilot schemes, the block-type pilot schemes provide the opportunity to protect the data with high importance/priority by transmitting them at the positions where the error rate is low. Therefore, comb-type pilot schemes are more suitable for generic data transmission, while the block-type pilot schemes are more suitable for transmission over slow fading channels or transmission with unequal error protection (UEP). Simulation results in [2,3,5,6] are plotted in this section.

In **Figure 3**, the symbol error rate (SER) versus the average SNR is plotted for the proposed block-type pilot channel estimation schemes over a slow fading channel with a bandwidth of 500 kHz, 16QAM modulation, DFT size $N = 64$, and a cyclic prefix $L = 4$. In this figure, the legends LS, MMSE, OLR-MMSE-5, and OLR-MMSE-25 present the estimators based on LS, MMSE, OLR-MMSE with rank $p = 5$ and OLR-MMSE with rank $p = 25$, respectively, without the decision feedback. The MMSE estimator yields the best performance, and LS yields the worst. Also, for the OLR-MMSE estimator, a SER floor is shown due to loss of channel information by reducing the rank of the channel correlation matrix.

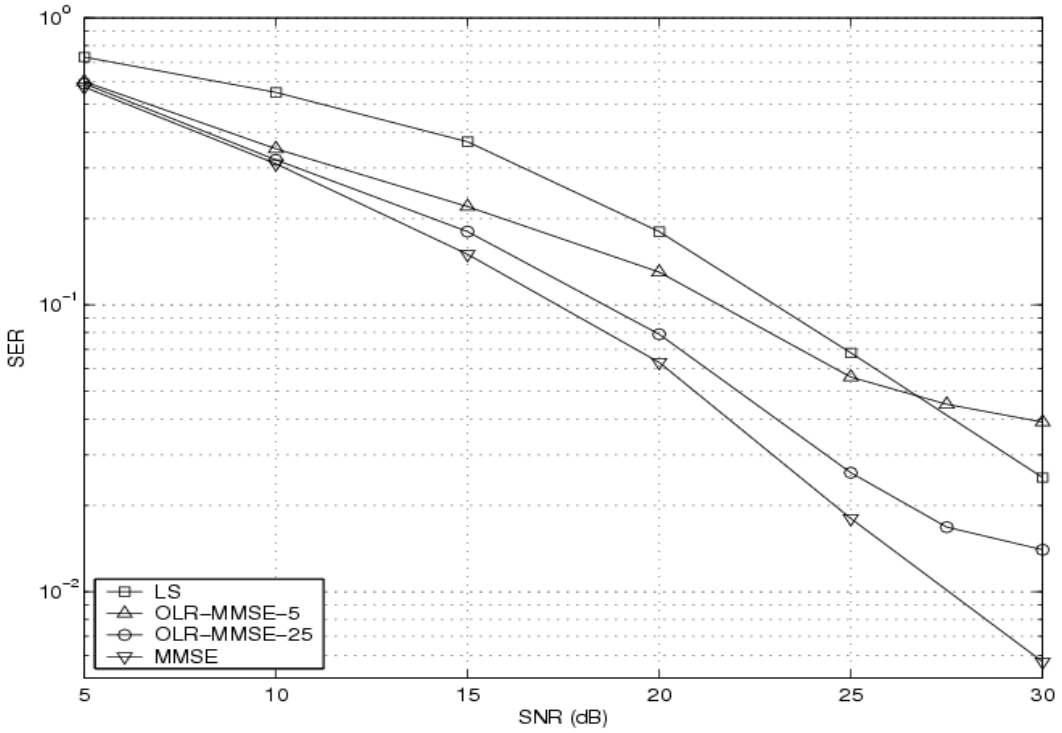

Figure 3. SER Performance versus SNR for Block-Type Pilot Channel Estimation Based on LS, MMSE, and OLR-MMSE algorithms

Figure 4 compares the SER performance of the estimation schemes with block-type pilot arrangement and comb-type pilot arrangement over a fast fading channel with Doppler frequency 70 Hz. The parameters are 17.5 kHz bandwidth, 16QAM modulation, DFT size $N = 1024$, the number of pilot subcarriers per symbol $N_p = 128$, and a cyclic prefix $L = 256$. In the figure, the legends B-LS, B-LS-FD represent the block-pilot channel estimation based on LS algorithm, with and without decision feedback, respectively; and the legends C-LI, C-SOI, C-TDI, C-SCI and C-LPI represent the comb-type pilot estimation based on LS algorithm, with the linear interpolation, the second order interpolation, the time domain interpolation, the spline cubic interpolation and the low-pass interpolation, respectively. The results show that the comb-type estimation schemes outperform block-type schemes, which is because the channel changes so fast that there are even changes for adjacent OFDM symbols. It is also shown that the performance among the comb-type estimation techniques usually ranges from the best to the worst as follows: low-pass, spline cubic, time-domain, second order, and linear.

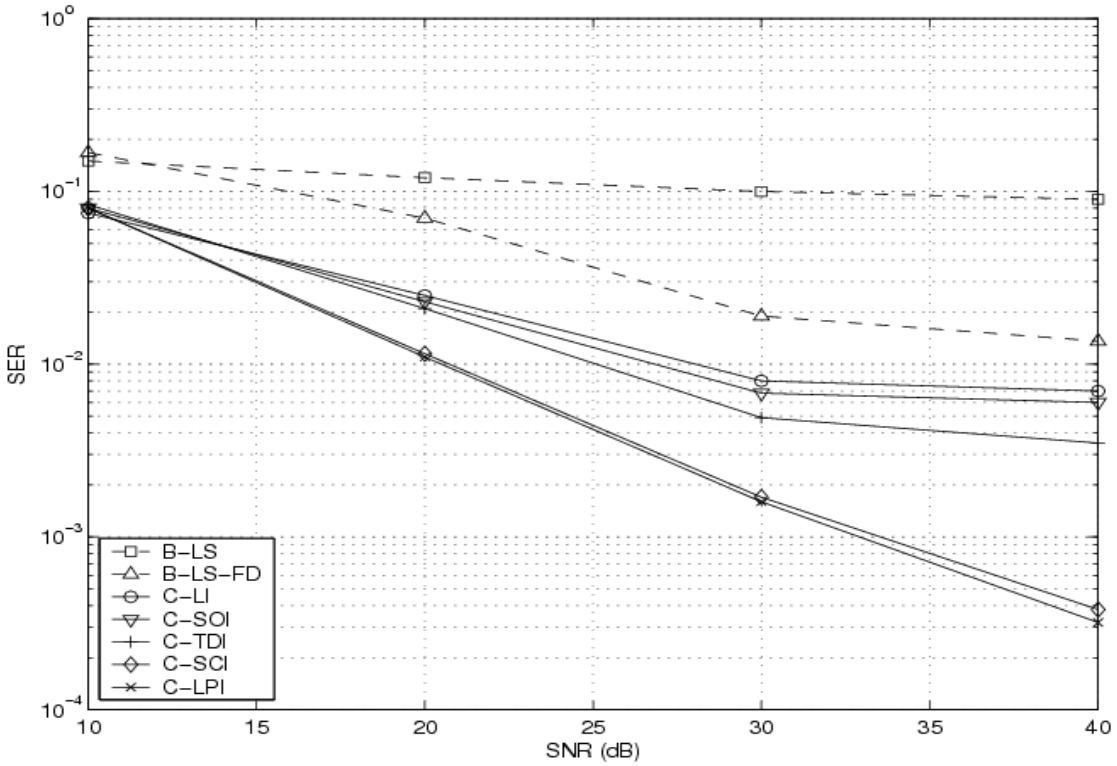

Figure 4. SER Performance versus SNR for the Channel Estimators Based On LS with Block-Type and Comb-Type Pilot Arrangements

Figure 5 shows the SER performance plotted for the three different estimators with comb-type pilot arrangement. A fast fading channel with a bandwidth 5 MHz consists of 6 independent resolvable paths (that is, $K = 6$). Other parameters are 16 QAM modulation, DFT size $N = 1024$, the number of pilot subcarriers per symbol $N_p = 32$, and a cyclic prefix $L = 16$. The legends LS-LPI, MLE, and PCMBE represent the LS estimator with low-pass interpolation, the ML estimator, and the PCMB estimator, respectively. Simulation results show that the performance of LS-LPI is worse than the other two, and the performance of PCMB is slightly better than MLE at small SNRs.

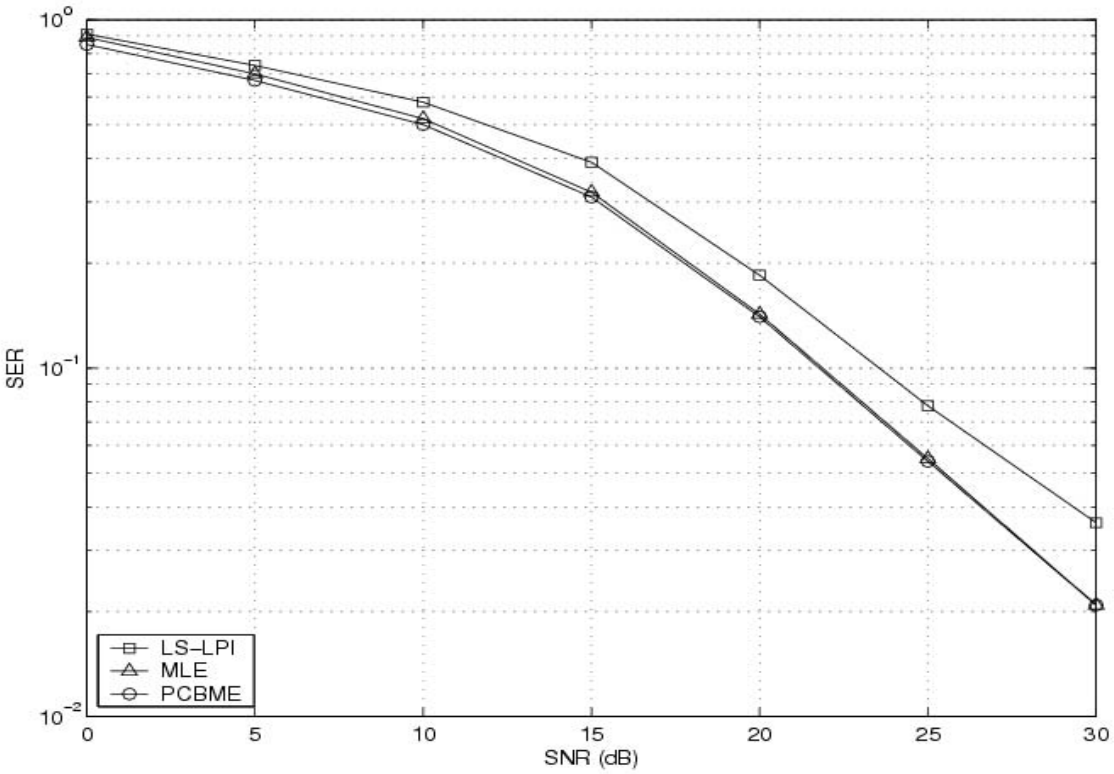

Figure 5. SER Performance versus SNR of the Comb-Type Pilot Channel Estimation with LS Estimator Using Low-Pass Interpolation, ML Estimator, and PCMB Estimator

7 Conclusions

In OFDM systems, efficient channel estimation schemes are essential for coherent detection of a received signal. After multi-carrier demodulation, the received signal is typically correlated in two dimensions, in time and frequency. By periodically inserting pilots in the time-frequency grid to satisfy the 2D sampling theorem, the channel response can be reconstructed by exploiting its correlation in time and frequency.

This paper fully reviews channel estimation strategies in OFDM systems. It describes block-type pilot-channel estimators, which may be based on least square (LS), minimum mean-square error (MMSE) or optimal low-rank MMSE (OLR-MMSE), with or without a decision feedback equalizer. It also analyzes the comb-type pilot channel estimators, which can be an LS estimator with certain 1D interpolation, the maximum likelihood (ML) estimator, or the parametric channel modeling-based (PCMB) estimator. Other channel estimators are introduced, such as the estimators based on 2D pilot arrangement with simplified 2D interpolation, the iterative estimators based on iterative filtering and decoding, and the estimators for the OFDM systems with multiple transmit antennas.

The mathematical analysis and the simulation results show that in comb-type pilot channel estimation, the LS estimator with low-pass interpolation (LPI) performs the best of all 1D interpolation methods, and it has a low computational complexity. The PCMB estimator yields the best performance among all comb-type pilot channel estimators, but it has a relatively higher complexity and larger processing delay. In block-type pilot channel estimation, the OLR-MMSE estimator with decision feedback equalizer gives the best tradeoff between performance and complexity. Block-type pilot channel estimation is more suitable for the slow fading channel conditions, while the comb-type pilot channel estimation usually outperforms for the middle and fast fading channels. The recommended channel estimation schemes for OFDM systems are summarized in **Table 3**.

Table 3. Recommended OFDM System Channel Estimation Schemes for Different Scenarios and Requirements

Scheme	Scenario	Pilot	Complexity	2nd Order Statistics of Channel	Performance
OLR-MMSE	Slow fading channel	Block-type	Moderate	Needed	Good
LS with LPI	Middle and fast fading channel	Comb-type	Low	Not needed	Good
PCMB			High	Needed	Very good

8 References

[1] Edfors, O., Sandell, M., Van de Beek, J.-J., Landström, D., and Sjöberg, F., *An Introduction to Orthogonal Frequency Division Multiplexing*, Luleå, Sweden: Luleå Tekniska Universitet, 1996, pp. 1–58.

[2] Van de Beek, J.-J., Edfors, O. S., Sandell, M., Wilson, S. K., and Börjesson, O. P., "On channel estimation in OFDM systems," *45th IEEE Vehicular Technology Conference*, Chicago, Il., vol. 2, pp. 815-819, July 1995.

[3] Edfors, O., Sandell, M., Van de Beek, J.-J., and Wilson, S. K., "OFDM Channel Estimation by Singular Value Decomposition," *IEEE Transactions on Communications*, vol. 46, pp. 931–939, July 1998.

[4] Strobach, P., "Low-Rank Adaptive Filters," *IEEE Transactions on Signal Processing*, vol. 44, pp. 2932–2947. Dec. 1996.

[5] Coleri, S., Ergen, M., Puri, A., and Bahai, A., "Channel Estimation Techniques Based on Pilot Arrangement in OFDM Systems," *IEEE Transactions on Broadcasting*, vol. 48, pp. 223–229, Sept. 2002.

[6] Wu, J., and Wu, W., "A Comparative Study of Robust Channel Estimators for OFDM Systems," *Proceedings of ICCT*, pp. 1932–1935, 2003.

[7] Yang, B., Letaief, K. B., Cheng, R. S., and Cao, Z., "Channel Estimation for OFDM Transmission in Multipath Fading channels Based on Parametric Channel Modeling," *IEEE Transactions on Communications*, vol. 49, pp. 467–479, March 2001.

[8] Ottersten, B., Viberg, M., and Kailath, T., "Performance Analysis of the Total Least Squares ESPRIT Algorithm," *IEEE Transactions on Signal Processing*, vol. 39, pp. 1122–1135, May 1991.

[9] Hou, X., Li, S., Liu, D., Yin, C., and Yue, G., **"**On Two-dimensional Adaptive Channel Estimation in OFDM Systems," *60th IEEE Vehicular Technology Conference*, Los Angeles, Ca., vol. 1, pp. 498–502, Sept. 2004.

[10] Sanzi, F., Sven, J., and Speidel, J., "A Comparative Study of Iterative Channel Estimators for Mobile OFDM Systems," *IEEE Transactions on Wireless Communications*, vol.2, pp. 849–859, Sept. 2003.

[11] Li, Y., "Simplified Channel Estimation for OFDM Systems with Multiple Transmit Antennas," *IEEE Transactions on Communications*, vol. 1, pp. 67-75, January 2002.

[12] Auer, G., "Channel Estimation in Two Dimensions for OFDM Systems with Multiple Transmit Antennas," *GLOBECOM*, pp. 322–326, 2003.

[13] IEEE P802.16 (Draft 8, May 2005), WiMAX Specification.

How to Reach Us:

Home Page:
www.freescale.com

E-mail:
support@freescale.com

USA/Europe or Locations not listed:
Freescale Semiconductor
Technical Information Center, CH370
1300 N. Alma School Road
Chandler, Arizona 85224
+1-800-521-6274 or +1-480-768-2130
support@freescale.com

Europe, Middle East, and Africa:
Freescale Halbleiter Deutschland GMBH
Technical Information Center
Schatzbogen 7
81829 München, Germany
+44 1296 380 456 (English)
+46 8 52200080 (English)
+49 89 92103 559 (German)
+33 1 69 35 48 48 (French)
support@freescale.com

Japan:
Freescale Semiconductor Japan Ltd.
Headquarters
ARCO Tower 15F
1-8-1, Shimo-Meguro, Meguro-ku,
Tokyo 153-0064, Japan
0120 191014 or +81 3 5437 9125
support.japan@freescale.com

Asia/Pacific:
Freescale Semiconductor Hong Kong Ltd.
Technical Information Center
2 Dai King Street
Tai Po Industrial Estate
Tai Po, N.T. Hong Kong
+800 2666 8080
support.asia@freescale.com

For Literature Requests Only:
Freescale Semiconductor Literature Distribution Center
P.O. Box 5405
Denver, Colorado 80217
1-800-441-2447 or 303-675-2140
Fax: 303-675-2150
LDCForFreescaleSemiconductor@hibbertgroup.com

AN3059
Rev. 0
1/2006

freescale semiconductor